UMCM#2503468, VOL 0, ISS 0

# Pull-in voltage of a circular nanoplate with elastically restrained edge subject to van der Waals attractions

E. Radi and G. Bianchi

## QUERY SHEET

This page lists questions we have about your paper. The numbers displayed at left are hyperlinked to the location of the query in the paper.

The title and author names are listed here as they will appear in your paper and the Table of Contents. Please check that this information is correct and let us know if any changes are needed. Also check that affiliations, funding information and conflict of interest statements are correct.

Please review your paper as a whole for typos and essential corrections. Note that we cannot accept a revised manuscript at this stage of production or major corrections, which would require Editorial review and delay publication.

## AUTHOR QUERIES

**Q1** Please resupply the corresponding author details if it is inaccurate.

**Q2** Figures citation as well as captions have been renumbered to maintain sequential order. Please check.

**Q3** There is no mention of Reference [37] in the text. Please cite the reference in the text. If no citation is supplied, we will delete the uncited reference from the list.

MECHANICS OF ADVANCED MATERIALS AND STRUCTURES
https://doi.org/10.1080/15376494.2025.2503468

Taylor & Francis
Taylor & Francis Group

ORIGINAL ARTICLE



# Pull-in voltage of a circular nanoplate with elastically restrained edge subject to van der Waals attractions

E. Radi[a,b] and G. Bianchi[c]

[a]Dipartimento di Scienze e Metodi dell'Ingegneria, Università di Modena and Reggio Emilia, Reggio Emilia, Italy; [b]Centro Interdipartimentale En&Tech, Reggio Emilia, Italy; [c]Dipartimento di Ingegneria e Architettura, Università di Parma, Parma, Italy

**ABSTRACT**

This work provides accurate analytic relations for the pull-in voltage of electrostatically actuated circular nanoplates with an elastically restrained edge, modeled according to the classic Kirchhoff thin plate theory taking into account the van der Waals attractive force. The cases of clamped or simply-supported edges are recovered as limit cases of the more realistic boundary conditions considered here. The electrostatic loading distribution is approximated by considering the deflection of the elastically restrained circular plate under a uniformly distributed transverse loading. The Green's functions of the plate under the elastically restrained boundary conditions are then used for calculating the deflection of the plate center due to the assumed loading distribution, which also depends on the deflection of the plate center. A closed-form nonlinear relation between the applied electrostatic loading and the deflection of the plate center is thus obtained, which displays a maximum at the pull-in voltage. The analytical model can also capture the effects of intermolecular attractions, which becomes relevant when the distance gap between the electrodes becomes of few nanometers. A comparison with the numerical and experimental results available in the literature for the limit case of clamped edge is then provided to assess the accuracy of the approximated analytical model.

**ARTICLE HISTORY**
Received 24 March 2025
Accepted 5 May 2025

**KEYWORDS**
Axisymmetric circular thin plate; pull-in instability; analytical model; van der Waals force; elastic constraint; MEMS and NEMS

## 1. Introduction

Micro- and nanoplates are basic structural components widely used in MEMS and NEMS devices with notable application as sensors and actuators. Applying a differential voltage between two electrodes, one connected to the plate and the other to the ground at a small distance from the plate, is the most common actuation principle due to its simplicity and high efficiency [1,2]. As the differential voltage between the electrodes increases, the plate deflects toward the fixed base electrode and consequently, the electrostatic attractive force acting on it also increases. Beyond a critical value of the applied voltage, the plate deflection becomes unstable and will cause the collapse of the nanoplate onto the fixed electrode [3–7]. An accurate investigation of this phenomenon, known as the pull-in instability, is fundamental to guarantee the effective design of reliable MEMS and NEMS devices. In Particular, investigating the pull-in behavior of electrostatically-actuated thin circular plates is essential for the correct design of micropumps, which are the main component used in drug delivery systems for accurately regulating very small volumes in several industrial, chemical, medical, and biomedical applications [8]. Such a nanoelectromechanical system is also the basic technology employed in the fabrication of capacitive microphones [9–11], energy harvesting systems [12,13], and many sensors and actuators. For these devices, it is crucial to accurately predict the occurrence of pull-in instability, as contact between the two electrodes can damage the device.

Owing to the number of applications in which they are involved, many studies on the pull-in instability of micro- and nanoplates have been performed in the literature, ranging from the simple 1-D lumped models, which impose significant limits on their accuracy [14,15], to more effective numerical and semi-analytical approaches [16]. The continuous model developed in Liao et al. [17] for circular thin plates is formulated through a fourth-order nonlinear partial differential equation according to the Kirchhoff theory of thin plates, whose solution is approximated by using the Galerkin method and assuming the first mode shape functions of the plate as trial functions. Moreover, the results are validated by comparison with finite element simulations and experiments. Nabian et al. [18] linearized the governing equation using a step-by-step linearization method and then solved the linear system of equations by the finite difference method. Ahmad and Pratap [19] used the Galerkin-weighted residual technique to solve the thin-plate electrostatic-elastic equation, by using the quasistatic deflection of the plate subject to a uniformly distributed loading as a trial function, which satisfies all the boundary conditions (BCs). A similar approach was recently adopted by Zabihi et al. [20] and

CONTACT Enrico Radi enrico.radi@unimore.it Dipartimento di Scienze e Metodi dell'Ingegneria, Università di Modena and Reggio Emilia, Reggio Emilia, Italy; Centro Interdipartimentale En&Tech, Reggio Emilia, Italy.

Supplemental data for this article can be accessed online at https://doi.org/10.1080/15376494.2025.2503468.

Havreland and Thomsen [21], where the investigation of circular nanoplates under electrostatic actuation was extended to consider the effects of nonlocal and strain gradient material behavior, in-plane prestress, and large deflection, respectively.

For reliable predictions of the pull-in voltage of circular nanoplates, the flexibility of the support must be taken into account properly. To this aim, rotationally restrained edges are more realistic BCs than the classical simply-supported and clamped edges. Moreover, the classical BCs can be recovered in the limiting case when the rigidity of the rotational constraint tends to zero or infinity. The effects of rotationally restrained edge on the pull-in voltage of micro- and nanobeams were investigated by Abadyan et al. [22] and Radi et al. [23], and a remarkable variation of the pull-in voltage with the rigidity of the rotational constraint was detected. While the effects of rotationally restrained edges on the dynamics and buckling of circular plates have been extensively investigated [24–26], the electrostatic response of circular plates with rotationally restrained edges is investigated here for the first time.

With respect to previous approaches, which are based on numerical or semi-analytical procedures, the present investigation provides an approximated but closed-form relation between the applied voltage and the central plate deflection of an electrostatically actuated circular nanoplate modeled according to the classic Kirchhoff thin plate theory, and subject to the van der Waals intermolecular force. The maximum value of this relation then yields the pull-in voltage and the corresponding plate deflection.

The boundary value problem is governed by a fourth order nonlinear ODE, and it can be equivalently formulated in terms of a nonlinear integral equation, whose kernel is the Green's function of the axisymmetric problem. As the electrostatic loading distribution acting on the plate depends on the plate deflection nonlinearly, an analytical solution is impractical, and an approximated solution is sought here. To obtain the closed-form approximate relation between the applied voltage and the deflection of the plate center, the loading distribution is calculated by considering the deflection of the plate under a uniformly distributed load, which causes the actual unknown deflection of the plate center. The Green's function of the plate elastically restrained at the edge under axisymmetric loading is then used for calculating the deflection of the plate center due to the assumed loading distribution.

The present approach may be seen as the first steps of an iterative analytical procedure. The starting point consists in assuming a preliminary shape function for the plate deflection used for calculating the electrostatic load acting on the plate. This preliminary shape function corresponds to a uniform load distribution, as that occurring for a negligible plate deflection. Then, the exact plate deflection caused by the calculated electrostatic load distribution is obtained by using the axisymmetrical Green's function for the circular plate. In this way, a closed-form nonlinear relation between the applied electrostatic loading and the deflection of the plate center is obtained, which displays a maximum at the pull-in voltage. A similar approach based on the use of Green's function was also exploited by Radi et al. [23,27,28] and by Bianchi and Radi [29], to define accurate analytical upper and lower bounds on the pull-in voltage of micro- and nanocantilevers and carbon nanotubes. The effects of the intermolecular attractions and flexibility of the elastic constraint are put in evidence and discussed. The special cases of simply-supported edge and clamped edge are derived in the limits of vanishing and infinitely large stiffness of the rotational spring, respectively. A comparison with numerical and experimental results available in the literature was then provided to assess the accuracy of the approximate analytical model, which defines a safe operation voltage regime for the device.

## 2. Governing nonlinear equations

A typical configuration of a micropump device based on the electrostatic actuation of a thin circular plate is illustrated in Figure 1. The architecture of the device consists of a thin circular plate electrode of radius $a$, and thickness $h$, separated by an initial gap distance $g$ from the fixed base electrode. The plate is supported along the edge and elastically restrained by a rotational spring of stiffness $k$.

A voltage difference $V$ applied between two electrodes generates an electrostatic attractive force causing radially symmetric deflection of the nanoplate. Let $u(r)$ represent the transverse deflection of the plate toward the fixed electrode, where $r$ is the radial coordinate taken from the plate center ($0 \le r \le a$).

The nonlinear ODE governing the problem of deflection of a thin circular plate under electrostatic actuation, obtained from the classical Kirchhoff plate theory, can then be written as [17,18].

$$u''''(r)+\frac{2}{r}u'''(r)-\frac{1}{r^2}u''(r)+\frac{1}{r^3}u'(r) = \frac{\varepsilon V^2}{2D\left[g-u(r)\right]^2}+\frac{A}{6\pi D\left[g-u(r)\right]^3}, \quad (1)$$

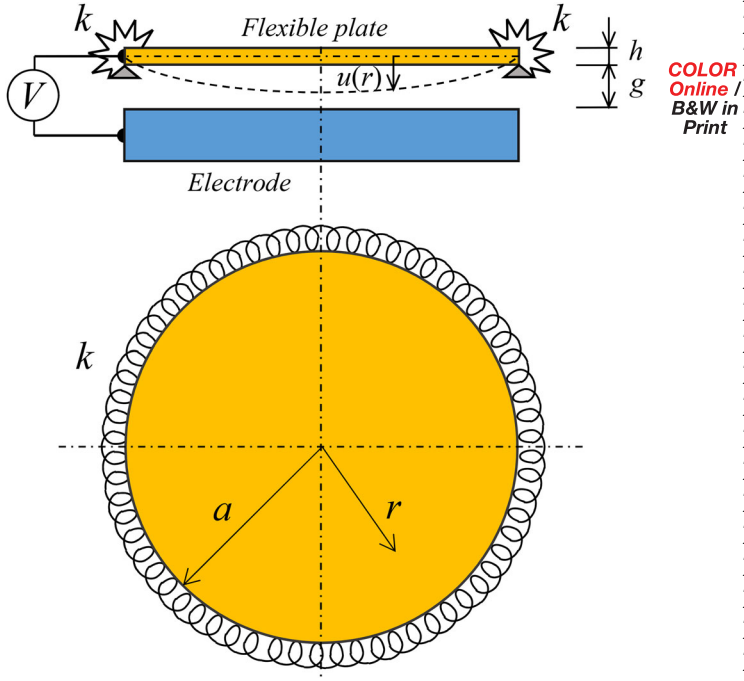


Figure 1. Schematic of the electrostatic actuation of a thin circular plate with elastically restrained edge by a rotational spring of stiffness $k$.

Where the prime denotes the derivative with respect to the argument within the brackets, $\varepsilon = 8.854\ 10^{-12}\ \mathrm{C}^2\ \mathrm{N}^{-1}\ \mathrm{m}^{-2}$ is the relative permittivity of the air, $A$ is the Hamaker constant which takes into account the material properties of the electrodes (for two identical metals interacting across vacuum (air) $A$ has values in range (3–5) $10^{-19}$ J [30]), and

$$D = \frac{Eh^3}{12(1-\nu^2)}, \tag{2}$$

Is the flexural rigidity of the plate, where $E$ is the Young modulus of elasticity and $\nu$ is the Poisson ratio.

The electrostatic force at the right end member of the ODE Eq. (1) provides an approximation of the capacitance between two parallel plates for which the fringing fields at the boundary are neglected.

Note that the Kirchhoff plate theory provides accurate results when the thickness of the plate is relatively small (i.e. for $1/10 < h/R < 1/20$) and the plate deflection is of the same order of the plate thickness.

The BCs are determined from the requirement of the radially symmetrical conditions at $r = 0$, namely

$$u'''(0) = 0, \quad u'(0) = 0, \tag{3}$$

And from the elastic restraint conditions along the supported edge of the circular plate at $r = a$, which require vanishing transversal displacement and a linear relation between the slope and the radial bending moment exerted by the rotational spring surrounding the plate, namely

$$u(a) = 0, \quad m_r(a) = k\ u'(a), \tag{4}$$

Where $k$ is the rotational stiffness of the elastically restrained boundary and

$$m_r = -D\left(u'' + \frac{\nu}{r}u'\right), \tag{5}$$

Is the bending moment per unit width along the radial direction.

By introducing the following nondimensional quantities:

$$\rho = \frac{r}{a}, \quad w = \frac{u}{g}, \quad \beta = \frac{\varepsilon V^2 a^4}{2Dg^3}, \quad \alpha_W = \frac{Aa^4}{6\pi Dg^4}, \quad \chi = \frac{ak}{D}, \tag{6}$$

The governing ODE Eq. (1) becomes

$$w''''(\rho) + \frac{2}{\rho}w'''(\rho) - \frac{1}{\rho^2}w''(\rho) + \frac{1}{\rho^3}w'(\rho) = \frac{\beta}{[1-w(\rho)]^2} + \frac{\alpha_W}{[1-w(\rho)]^3} \tag{7}$$

And the BCs Eqs. (3) and (4) require

$$\begin{gathered} w'(0) = 0, \\ w'''(0) = 0, \\ w(1) = 0, \\ w''(1) + (\nu + \chi)\ w'(1) = 0. \end{gathered} \tag{8}$$

Note that the limit cases of a simply-supported circular plate (SSCP) and a clamped circular plate (CCP) are recovered for $\chi = 0$ and $\chi \to \infty$, respectively.

### 2.1. Green's functions for an elastically restrained circular plate

The Green's function $G(\rho, t)$ for an elastically restrained circular plate under axisymmetric loading is the plate deflection at radial coordinate $\rho$ due to a line load distributed along the circle of radius $t$, namely the solution of the following ODE [31]:

$$\frac{\partial^4 G}{\partial \rho^4} + \frac{2}{\rho}\frac{\partial^3 G}{\partial \rho^3} - \frac{1}{\rho^2}\frac{\partial^2 G}{\partial \rho^2} + \frac{1}{\rho^3}\frac{\partial G}{\partial \rho} = \delta(\rho - t), \tag{9}$$

Where $\delta$ denotes the Dirac delta function, subject to the same BCs Eq. (8) on the function $G$ and to the following continuity conditions at $\rho = t$:

$$\begin{gathered} G(t^+, t) = G(t^-, t), \quad G'(t^+, t) = G'(t^-, t), \\ G''(t^+, t) = G''(t^-, t), \quad G'''(t^+, t) - G'''(t^-, t) = 1. \end{gathered} \tag{10}$$

By imposing the BCs Eq. (8) on the function $G$ and the continuity conditions Eq. (10), the Green's function for an elastically restrained circular plate of unit radius can be univocally determined as

$$G(\rho, t) = \begin{cases} \left[(1-t^2)\dfrac{3+\nu+\chi-(1-\nu-\chi)\ \rho^2}{1+\nu+\chi} + (\rho^2+t^2)\ln t^2\right]\dfrac{t}{8}, & \text{for} \quad 0 \le \rho < t, \\ \left[(1-\rho^2)\dfrac{3+\nu+\chi-(1-\nu-\chi)\ t^2}{1+\nu+\chi} + (\rho^2+t^2)\ln r^2\right]\dfrac{t}{8}, & \text{for} \quad t < \rho \le 1. \end{cases} \tag{11}$$

Thus, the BVP formed by the ODE Eq. (7) and the BCs Eq. (8) can be equivalently formulated in terms of the following nonlinear integral equation

$$\begin{aligned} w(\rho) = {} & \frac{1}{8}\int_0^\rho \left[(1-\rho^2)\frac{3+\nu+\chi-(1-\nu-\chi)\ t^2}{1+\nu+\chi} + (\rho^2+t^2)\ln \rho^2\right] \\ & \left\{\frac{\beta}{[1-w(t)]^2} + \frac{\alpha_W}{[1-w(t)]^3}\right\} t\,dt + \\ & \frac{1}{8}\int_\rho^1 \left[(1-t^2)\frac{3+\nu+\chi-(1-\nu-\chi)\ \rho^2}{1+\nu+\chi} + (\rho^2+t^2)\ln t^2\right] \\ & \left\{\frac{\beta}{[1-w(t)]^2} + \frac{\alpha_W}{[1-w(t)]^3}\right\} t\,dt \end{aligned} \tag{12}$$

Therefore, the deflection $w_0$ at the center of the plate ($\rho = 0$) is given by

$$w_0 = \frac{1}{8}\int_0^1 \left[\frac{3+\nu+\chi}{1+\nu+\chi}(1-t^2)+t^2\ln t^2\right] \left\{\frac{\beta}{[1-w(t)]^2}+\frac{\alpha_W}{[1-w(t)]^3}\right\} tdt. \tag{13}$$

## 3. Approximated pull-in voltage

To work out an approximated relation between the nondimensional voltage parameter $\beta$ and nondimensional deflection $w_0$, we introduce the deflection generated by a uniformly distributed loading on the plate that causes the deflection $w_0$ of the plate center at the right-hand sides of Eq. (12).

The normalized deflection of an elastically restrained circular plate subject to a uniformly distributed load $p$, which satisfies the BCs Eq. (8), is given by

$$w(\rho) = \frac{p}{8}\int_0^\rho \left[(1-\rho^2)\frac{3+\nu+\chi-(1-\nu-\chi)\ t^2}{1+\nu+\chi}+(\rho^2+t^2)\ln\rho^2\right] tdt + \frac{p}{8}\int_\rho^1 \left[(1-t^2)\frac{3+\nu+\chi-(1-\nu-\chi)\ \rho^2}{1+\nu+\chi}+(\rho^2+t^2)\ln t^2\right] tdt, \tag{14}$$

Namely [24]

$$w(\rho) = \frac{p}{64}(1-\rho^2)\left(1-\rho^2+\frac{4}{1+\nu+\chi}\right). \tag{15}$$

Therefore, the deflection caused by a uniformly distributed load $p$ that causes the deflection $w_0$ of the plate center is

$$w(\rho) = w_0(1-\rho^2)(1-c\rho^2). \tag{16}$$

Where $w_0$ is the normalized deflection of the plate center produced by the distributed load $p$ ($w_0 < 1$), and

$$c = \frac{1+\nu+\chi}{5-\nu+\chi}. \tag{17}$$

Therefore, we can assume $1/3 < c < 1$. By introducing the approximate deflection Eqs. (16) in (13), we obtain the following approximated nonlinear relations between the nondimensional parameters $\beta$ and $w_0$:

$$\beta = \frac{16w_0 - \alpha_W \int_0^1 \frac{(1-\tau)b+\tau\ln\tau}{[1-w_0(1-\tau)(1-c\ \tau)]^3}d\tau}{\int_0^1 \frac{(1-\tau)b+\tau\ln\tau}{[1-w_0(1-\tau)(1-c\ \tau)]^2}d\tau}, \tag{18}$$

Where the substitution $\tau = t^2$ has been introduced and

$$b = \frac{3+\nu+\chi}{1+\nu+\chi}. \tag{19}$$

The integrals in Eq. (18) have been calculated in closed-form, thus obtaining the following accurate analytical results:

$$\int_0^1 \frac{(1-\tau)b+\tau\ln\tau}{[1-w_0(1-\tau)(1-c\ \tau)]^2}d\tau = \frac{1}{w_0^2\ z^2}\left\{\frac{1+c}{1-w_0}bw_0+\frac{1-c}{z}b\ln\frac{1-(c-z)^2}{1-(c+z)^2}-\ln(1-w_0) +\frac{1+c}{z}\left[\mathrm{Li}_2\left(\frac{2c}{1+c-z}\right)-\mathrm{Li}_2\left(\frac{2c}{1+c+z}\right)\right]\right\}, \tag{20}$$

$$\int_0^1 \frac{(1-\tau)b+\tau\ln\tau}{[1-w_0(1-\tau)(1-c\ \tau)]^3}d\tau = \frac{1}{w_0^3\ z^5}\left\{\left[3bc\ (1-c)+\frac{(1+c)w_0\ z^2}{4(1-w_0)}\right]\ln\frac{1-(c-z)^2}{1-(c+z)^2} +3c(1+c)\left[\mathrm{Li}_2\left(\frac{2c}{1+c-z}\right)-\mathrm{Li}_2\left(\frac{2c}{1+c+z}\right)\right]\right\} + \frac{1}{2(1-w_0)w_0^2\ z^2}\times\left\{\frac{6bc\ (1+c)}{z^2}+b\frac{c+w_0}{1-w_0}w_0+w_0 +\left[\frac{3(1-c)^2}{2z^2}-1\right]\ln(1-w_0)\right\}. \tag{21}$$

Where

$$z = \sqrt{(1-c)^2+4c/w_0}, \tag{22}$$

And $\mathrm{Li}_2$ denotes the dilogarithm function [32], namely $\mathrm{Li}_2(x) = \Sigma_{k=1,\infty}\ x^k/k^2$.

## 4. Results and discussion

The approximate relations between the nondimensional electrostatic loading parameter $\beta$ and the nondimensional deflection of the plate center $w_0$ are plotted in Figure 2 according to Eq. (18), for six values of relative rotational stiffness $\chi$, four values of the van der Waals force, and $\nu = 0.3$.

These plots show a nonlinear increase of the applied voltage with the deflection of the plate center, which attains a maximum at about $w_0 = 0.45$ in the absence of intermolecular attractions, namely for $\alpha_W = 0$, and for smaller deflections when the van der Waals force is considered. The maximum voltage $\beta^*$ and the corresponding deflection of the plate center $w_0{}^*$ define the limit of the stable device response. They identify the pull-in voltage and pull-in deflection, respectively. The device behavior is stable for plate deflection lower than the critical one $w_0{}^*$, and it becomes instable when $\beta = \beta^*$ and $w_0 = w_0{}^*$. As the restraint stiffness increases, a high electrostatic voltage is required for deflecting the plate and the pull-in voltage increases correspondingly, see also Figure 3 which provides the variations of $\beta^*$ and $w_0{}^*$ with the relative rotational stiffness $\chi$, for four values of the van der Waals force. The Poisson ratio $\nu$ has a negligible influence on the pull-in

COLOR Online / B&W in Print

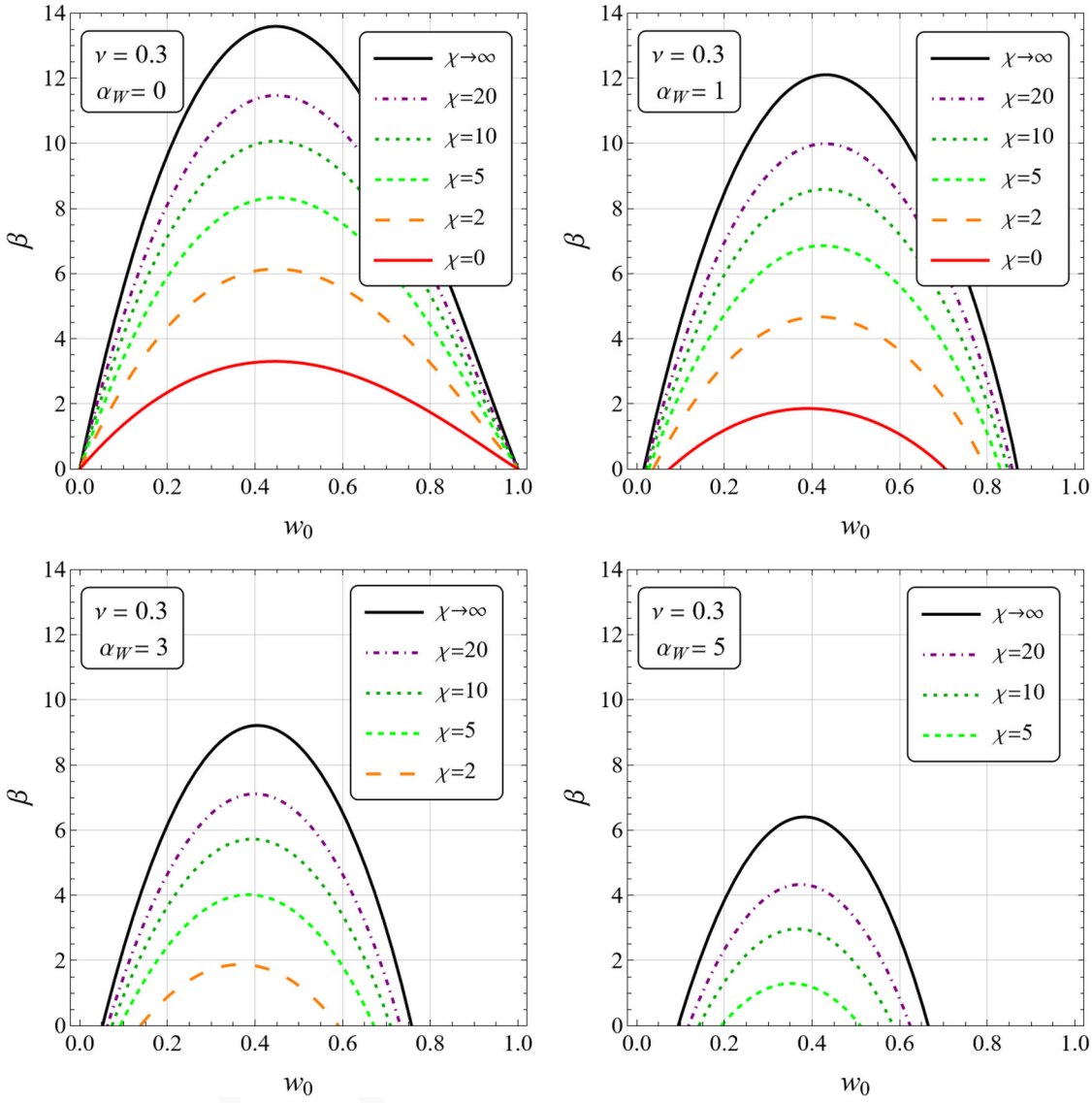


**Figure 2.** Approximate relations between the nondimensional electrostatic loading parameter $\beta$ and the nondimensional deflection of the plate center $w_0$ for some values of the relative rotational stiffness $\chi$ and van der Waals parameter $\alpha_W$.

COLOR Online / B&W in Print

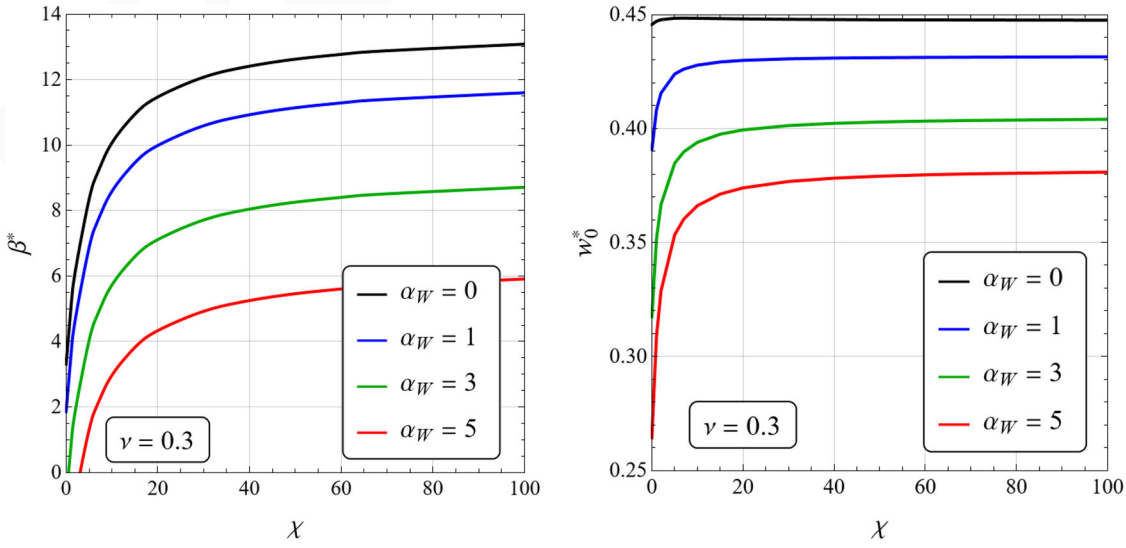


**Figure 3.** Approximated variation of the approximated pull-in parameters $\beta^*$ and $w_0^*$ with $\chi$, for $\nu = 0.3$, for four values of the van der Waal parameter $\alpha_W$.

voltage, except for small values of $\chi$. Therefore, we only considered the value $\nu = 0.3$ in Figures 2 and 3. A limited influence of the Poisson ratio is observed on the pull-in deflection $w_0{}^*$ as it can be observed in Figure 4 where the variations of the pull-in deflection of the plate center $w_0{}^*$ with the relative rotational stiffness $\chi$, are plotted for three values of the Poisson ratio $\nu$, in the absence of intermolecular forces ($\alpha_W = 0$). In particular, the latter results show that the pull-in deflection is almost constant for large values of the rotational stiffness $\chi$, and it has a limited range of variation as $\chi$ tends to 0.

In the following, we investigate the two limit cases of CCP and SSCP, which are recovered as $\chi \to \infty$ and $\chi \to \infty$, respectively.

The approximate relations between the nondimensional electrostatic loading parameter $\beta$ and the nondimensional deflection of the plate center $w_0$ are plotted in Figure 2*a* for $\nu = 0.3$ and for six values of relative rotational stiffness $\chi$, according to Eq. (18). These plots show a nonlinear increase of the applied voltage with the deflection of the plate center, which attains a maximum at about $w_0 = 0.45$.

This maximum voltage $\beta^*$ and the corresponding deflection of the plate center $w_0{}^*$ define the limits of the stable device response. They identify the pull-in voltage and pull-in deflection, respectively. As the restraint stiffness increases, a high electrostatic voltage is required for deflecting the plate and the pull-in voltage increases correspondingly, see also Figure 2*b* which provides the variation of $\beta^*$ with the relative rotational stiffness $\chi$. The Poisson ratio $\nu$ has a negligible influence on the pull-in voltage, except for small values of $\chi$. Therefore, we only considered the value $\nu = 0.3$ in Figure 2. The corresponding variations of the pull-in deflection of the plate center $w_0{}^*$ with the restraining parameter $\chi$ are plotted in Figure 3 for three values of the Poisson ratio $\nu$. These results show that the pull-in deflection is almost constant for large values of the rotational stiffness $\chi$, and it has a limited range of variation as $\chi$ tends to 0.

In the following, we investigate the two limit cases of CCP and SSCP, which are recovered as $\chi \to \infty$ and $\chi \to \infty$, respectively.

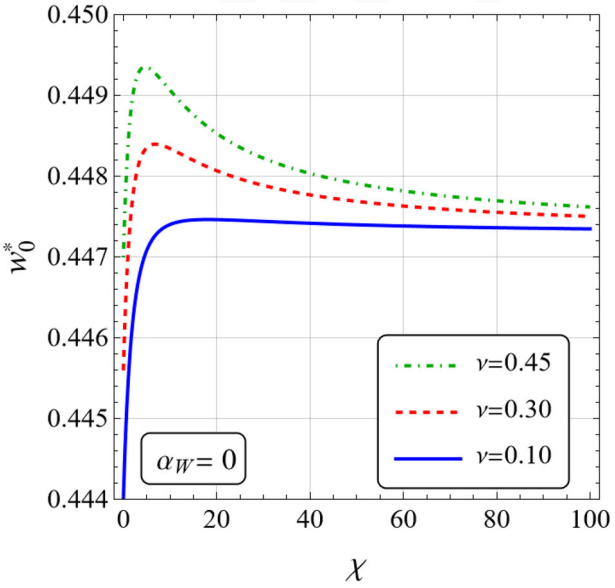


COLOR Online / B&W in Print

**Figure 4.** Variations of the approximated pull-in deflection of the plate center $w_0{}^*$ with the relative rotational stiffness $\chi$, for three values of the Poisson ratio $\nu$, in the absence of intermolecular forces ($\alpha_W = 0$).

## 5. Limiting cases and validation of results

For a CCP, namely for $\chi \to \infty$, by using the result (A.7), relation Eq. (18) provides

$$\beta = \frac{64w_0^2(1-w_0) - \frac{\alpha_W}{4}\left[2w_0\frac{5-3w_0}{1-w_0} - (2-3w_0)\ln(1-w_0) - \sqrt{w_0}\ln\frac{1+\sqrt{w_0}}{1-\sqrt{w_0}} + 3(1-w_0)\ \mathrm{L}(w_0)\right]}{2w_0 + (1-w_0)[\mathrm{L}(w_0) - \ln(1-w_0)]}, \tag{20}$$

Where

$$\mathrm{L}(w_0) = \sqrt{w_0}\left[\mathrm{Li}_2\left(\frac{\sqrt{w_0}}{\sqrt{w_0}-1}\right) - \mathrm{Li}_2\left(\frac{\sqrt{w_0}}{\sqrt{w_0}+1}\right)\right]. \tag{21}$$

### 5.1. Pull-in voltage in the absence of intermolecular attraction

In the absence of intermolecular attraction, namely for $\alpha_W = 0$, from Eq. (20) the maximum of the nondimensional voltage parameter $\beta$ for a CCP is attained at the nondimensional deflection $w_0{}^* = 0.4473$ and is given by $\beta^* = 13.587$. This value corresponds to the solid red curve in Figure 5, which turns out to be a bit lower than the experimental results obtained by [33] in his PhD thesis for a microplate with thickness $h = 3\,\mu\mathrm{m}$ and gap distance $g = 1\,\mu\mathrm{m}$. Therefore, the present analytical results for the pull-in voltage seem to be conservative. The present investigation indeed takes into account for the nonlinearity of the electrostatic force, but it neglects the nonlinear spring hardening due to the stiffening effect of the inplane tension occurring for large plate deflection [34–36], specially for thin plates. The conservative reduction of the predicted pull-in voltage with respect to the experimental results observed in Figure 5 may thus be a consequence of neglecting this peculiar stiffening contribution.

Using the finite difference method [18], found a bit larger nondimensional pull-in voltage, namely $\beta^* = 13.745$. Using a fifth-order Taylor series expansion method [17], proposed the following approximated value for the pull-in voltage of a CCP:

$$V^* = 5.4286\sqrt{\frac{Dg^3}{\varepsilon a^4}}, \tag{22}$$

Which yields $\beta^* = 14.735$. The related pull-in deflection is $w_0{}^* = 0.415$.

Using the Galerkin-weighted residual technique, Ahmad and Pratap [19] obtained the approximated pull-in voltage $\beta^* = 14.287$, and proposed the following analytical relation

$$V^* = 5.46\sqrt{\frac{D\ g^3}{\varepsilon\ a^4}}. \tag{23}$$

For a SSCP, namely for $\chi = 0$, and $\alpha_W = 0$, Eq. (18) yields

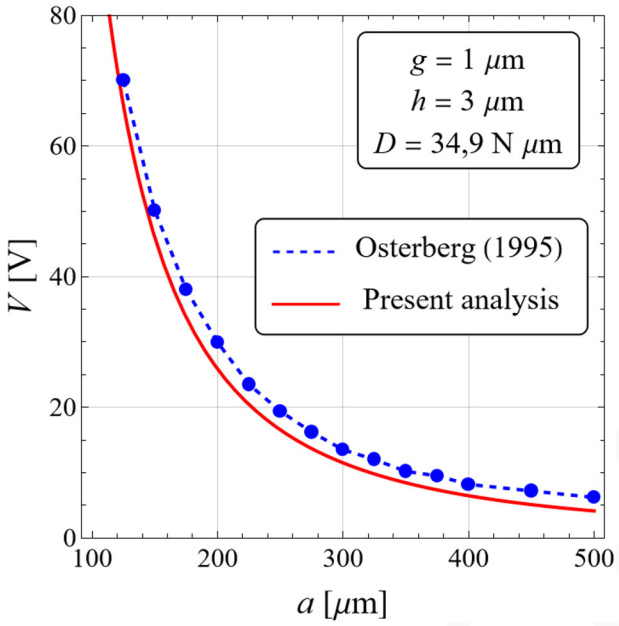


COLOR Online / B&W in Print

**Figure 5.** Variations of the pull-in voltage of a CCP with the plate radius $a$, in the absence of intermolecular forces ($\alpha_W = 0$): experimental results and approximated analytical results.

$$\beta = \frac{64\ \varphi^3 w_0^3}{(5-\nu)^2}\left\{3\ \mathrm{Li}_2\left(-\frac{1+\nu}{\varphi-3}\right) - 3\ \mathrm{Li}_2\left(\frac{1+\nu}{\varphi+3}\right)\right.$$

$$-\varphi \ln(1-w_0) + \frac{3+\nu}{1+\nu}\left[\frac{6\ w_0\ \varphi}{(1-w_0)(5-\nu)} + (2-\nu)\right.$$

$$\left.\left.\ln\frac{5-\nu-w_0(2-\nu+\varphi)}{5-\nu-w_0(2-\nu-\varphi)}\right]\right\}^{-1}, \tag{24}$$

Where

$$\varphi = \sqrt{(2-\nu)^2 + (5-\nu)(1+\nu)/w_0}. \tag{25}$$

The variation of the nondimensional voltage parameter $\beta$ given by the analytical relation Eq. (24) is plotted in Figure 6*a* for three different values of the Poisson coefficient.

The maximum nondimensional voltage parameter $\beta^*$ is calculated numerically from the analytical relation Eq. (24) and then plotted in Figure 6*b* as a function of the Poisson coefficient. Moreover, the following simple linear variation is found to approximate the variation of $\beta^*$ with the Poisson coefficient

$$\beta* = 2.68 + 2.04\nu, \tag{26}$$

Which holds for $0 \leq \nu < 0.5$. From the approximation Eq. (26) and Figure 6*b*, it can be observed that the pull-in voltage for a SSCP circular plate increases with the Poisson coefficient, while the approximated pull-in voltage for a CCP is found to be independent of the Poisson coefficient.

## 6. Conclusions

This work provides an approximated closed-form relation between the electrostatic voltage applied to a circular

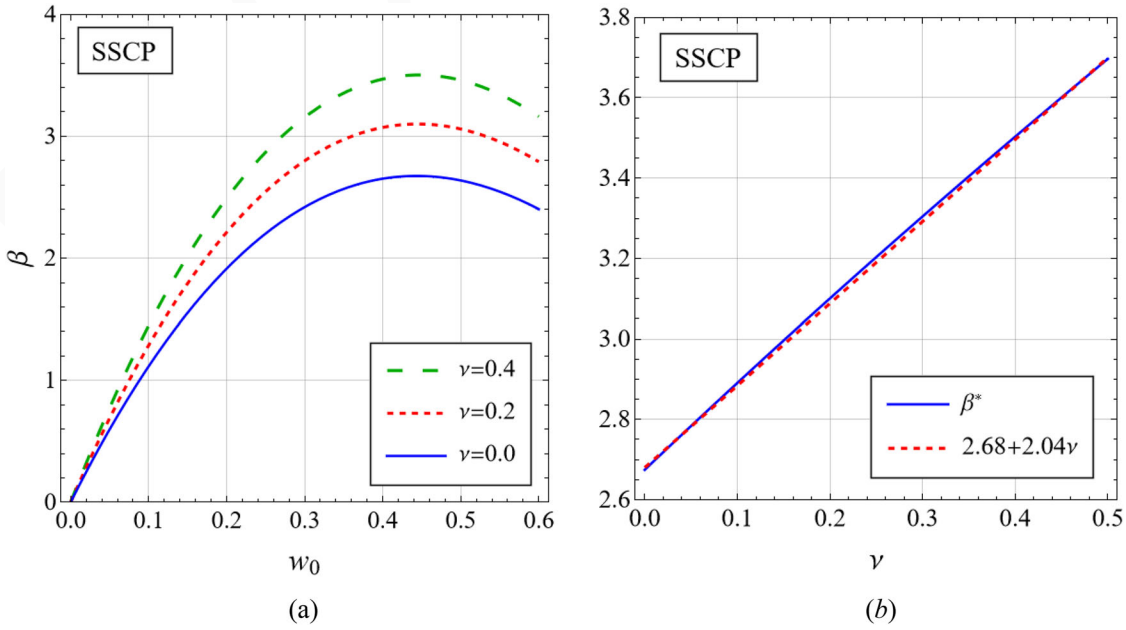


COLOR Online / B&W in Print

**Figure 6.** (*a*) Approximate relation between the nondimensional electrostatic loading parameter $\beta$ and the nondimensional deflection of the plate center $w_0$ for three values of the Poisson coefficient, (*b*) variation of the approximated pull-in voltage parameter $\beta^*$ with the Poisson coefficient (blue solid line) and approximated linear variation Eq. (26) (dashed red line) for a SSCP.

nanoplate elastically constrained against rotation at its edge and the deflection of the nanoplate center, by considering also the effects of the van der Waals intermolecular attractions, which become relevant at the nanoscale. The classical BCs of clamped or simply-supported edges are recovered in the limit case of infinite or vanishing rotational stiffness, respectively. We proposed an accurate analytical model of the switching system under electrostatic actuation, based on the Green's function for a circular plate elastically restrained against rotation along the edge, under axisymmetric loading. Then, we used this model to derive a closed-form approximated relation for the pull-in voltage that is convenient for the accurate design and optimization of MEMS and NEMS devices. It allows for estimating the pull-in voltage and deflection in advance, so that designers can ensure that the device operates in agreement with the specification requirements.

The results display a significant influence of the constraint rotational stiffness as well as the van der Waals attraction on the critical pull-in voltage and tip deflection. Moreover, they show close agreement with the numerical solutions presented in the literature for estimating the pull-in voltage of a CCP, thus validating the effectiveness of the proposed method. A sensible reduction of the predicted pull-in voltage with respect to experimental results is observed, specially for thin plates, which may be due to the stiffening effect of the inplane tension here neglected. No pull-in voltage predictions or experimental results can be found in the literature for an elastically restrained circular plate or a SSCP. The results obtained here also show that the pull-in voltage of a SSCP increases almost linearly with the Poisson coefficient $\nu$. All these findings can be useful for the accurate preliminary design of many MEMS and NEMS switch devices.

## Disclosure statement

No potential conflict of interest was reported by the author(s).

## Funding

Financial support within the framework of the grant PRIN 2022 PNRR "Energy harvesting *via* naturally induced piezoelectric vibration with a view toward application" [prot. P2022ATTAR; CUP B53D23026940001] is gratefully acknowledged.

## References

[1] V.M. Varadan, K.J. Vinoy, and K.A. Jose, RF MEMS and Their Applications, Wiley, New York, 2003.

[2] C.C. Liu, and C.K. Chen, Modeling and simulation of nonlinear micro-electromechanical circular plate, Smart Sci., vol. 1, no. 1, pp. 59–63, 2013. DOI: 10.1080/23080477.2013.11665587.

[3] R.C. Batra, M. Porfiri, and D. Spinello, Reduced-order models for microelectromechanical rectangular and circular plates incorporating the Casimir force, Int. J. Solids Struct., vol. 45, no. 11–12, pp. 3558–3583, 2008. DOI: 10.1016/j.ijsolstr.2008.02.019.

[4] F.C. Rahim, A numerical approach to investigate of pull-in phenomenon of circular micro plate subjected to nonlinear electrostatic pressure, Sens. Transducers., vol. 117, no. 6, pp. 41–49, 2010a.

[5] F.C. Rahim, Investigation effect of residual stress on pull-in voltage of circular micro plate subjected to nonlinear electrostatic force, Sens. Transducers., vol. 123, no. 12, pp. 25–34, 2010b.

[6] R. Ansari, R. Gholami, M.F. Shojaei, V. Mohammadi, and M.A. Darabi, Surface stress effect on the pull-in instability of hydrostatically and electrostatically actuated rectangular nanoplates with various edge supports, Mater. Technol., vol. 134, no. 4, pp. 041013, 2012.

[7] R. Ansari, R. Gholami, M.F. Shojaei, V. Mohammadi, and S. Sahmani, Surface stress effect on the pull-in instability of circular, Acta Astronaut., vol. 102, pp. 140–150, 2014. DOI: 10.1016/j.actaastro.2014.05.020.

[8] A. Nisar, N. Afzulpurkar, B. Mahaisavariya, and A. Tuantranont, MEMS-based micropumps in drug delivery and biomedical applications, Sens. Actuat. B: chem., vol. 130, no. 2, pp. 917–942, 2008. DOI: 10.1016/j.snb.2007.10.064.

[9] H. Gharaei, and J. Koohsorkhi, Design and characterization of high sensitive MEMS capacitive microphone with fungous coupled diaphragm structure, Microsyst. Technol., vol. 22, no. 2, pp. 401–411, 2016. DOI: 10.1007/s00542-014-2406-2.

[10] H.C. Her, T.L. Wu, and J.H. Huang, Acoustic analysis and fabrication of microelectromechanical system capacitive microphones, J. Appl. Phys., vol. 104, pp. 084509, 2008.

[11] M. Saadatmand, and J. Kook, Multi-objective optimization of a circular dual back-plate MEMS microphone: tradeoff between pull-in voltage, sensitivity and resonance frequency, Microsyst. Technol., vol. 25, no. 8, pp. 2937–2947, 2019. DOI: 10.1007/s00542-018-4240-4.

[12] X. Guo, Y. Zhang, K. Fan, C. Lee, and F. Wang, A comprehensive study of non-linear air damping and "pull-in" effects on the electrostatic energy harvesters, Energy Convers. Manag., vol. 203, pp. 112264, 2020.

[13] X. Ji, Nonlinear electromechanical analysis of axisymmetric thin circular plate based on flexoelectric theory, Sci. Rep., vol. 11, no. 1, pp. 21762, 2021. DOI: 10.1038/s41598-021-01289-0.

[14] J. Cheng, J. Zhe, and X.T. Wu, Analytical and finite element model pull-in study of rigid and deformable electrostatic microactuators, J. Micromech. Microeng., vol. 14, no. 1, pp. 57–68, 2004. DOI: 10.1088/0960-1317/14/1/308.

[15] R. Nadal-Guardia, A.M. Brosa, and A. Dehl, AC transfer function of electrostatic capacitive sensors based on the 1-D equivalent model: application to silicon microphones, J. Microelectromech. Syst., vol. 12, no. 6, pp. 972–978, 2003. DOI: 10.1109/JMEMS.2003.820290.

[16] G.W.V. Vogl, and A.H. Nayfeh, A reduced-order model for electrically actuated clamped circular plates, J. Micromech. Microeng., vol. 15, no. 4, pp. 684–690, 2005. DOI: 10.1088/0960-1317/15/4/002.

[17] L.D. Liao, P.C.P. Chao, C.W. Huang, and C.W. Chiu, DC dynamic and static pull-in predictions and analysis for electrostatically actuated clamped circular micro-plates based on a continuous model, J. Micromech. Microeng., vol. 20, no. 2, pp. 025013, 2010. DOI: 10.1088/0960-1317/20/2/025013.

[18] A. Nabian, G. Rezazadeh, M. Haddad-Derafshi, and A. Tahmasebi, Mechanical behavior of a circular micro plate subjected to uniform hydrostatic and non-uniform electrostatic pressure, Microsyst. Technol., vol. 14, no. 2, pp. 235–240, 2007. DOI: 10.1007/s00542-007-0425-y.

[19] B. Ahmad, and R. Pratap, Elasto-electrostatic analysis of circular microplates used in capacitive micromachined ultrasonic transducers, IEEE Sens. J., vol. 10, no. 11, pp. 1767–1773, 2010. DOI: 10.1109/JSEN.2010.2049017.

[20] A. Zabihi, R. Ansari, J. Torabi, F. Samadani, and K. Hosseini, An analytical treatment for pull-in instability of circular nanoplates based on the nonlocal strain gradient theory with clamped boundary condition, Mater. Res. Express., vol. 6, no. 9, pp. 0950b3, 2019. DOI: 10.1088/2053-1591/ab31bc.

[21] A.S. Havreland, and E.V. Thomsen, Analytical deflection profiles and pull-in voltage calculations of prestressed electrostatic

actuated MEMS structures, J. Microelectromech. Syst., vol. 30, no. 4, pp. 659–667, 2021. DOI: 10.1109/JMEMS.2021.3083935.

[22] M.R. Abadyan, Y.T. Beni, and A. Noghrehabadi, Investigation of elastic boundary condition on the pull-in instability of beam-type NEMS under van der Waals attraction, Proc. Eng., vol. 10, pp. 1724–1729, 2011. DOI: 10.1016/j.proeng.2011.04.287.

[23] E. Radi, G. Bianchi, and L. di Ruvo, Upper and lower bounds for the pull-in parameters of a micro- or nanocantilever on a flexible support, Int. J. Non-Linear Mech., vol. 92, pp. 176–186, 2017. DOI: 10.1016/j.ijnonlinmec.2017.03.011.

[24] C.L. Kantham, Bending and vibration of elastically restrained circular plates, J. Franklin Inst., vol. 265, no. 6, pp. 483–491, 1958. DOI: 10.1016/0016-0032(58)90393-4.

[25] W.P. Rdzanek, W.J. Rdzanek, and Z. Engel, Theoretical analysis of sound radiation of an elastically supported circular plate, J. Sound Vib., vol. 265, no. 1, pp. 155–174, 2003. DOI: 10.1016/S0022-460X(02)01445-1.

[26] A. Zagrai, and D. Donskoy, A soft table for the natural frequencies and modal parameters of uniform circular plates with elastic edge support, J. Sound Vib., vol. 287, no. 1-2, pp. 343–351, 2005. DOI: 10.1016/j.jsv.2005.01.021.

[27] E. Radi, G. Bianchi, and L. di Ruvo, Analytical bounds for the electro-mechanical buckling of a compressed nanocantilever, Appl. Math. Model., vol. 59, pp. 571–582, 2018. DOI: 10.1016/j.apm.2018.02.007.

[28] E. Radi, G. Bianchi, and A. Nobili, Bounds to the pull-in voltage of a MEMS/NEMS beam with surface elasticity, Appl. Math. Model., vol. 91, pp. 1211–1226, 2021. DOI: 10.1016/j.apm.2020.10.031.

[29] G. Bianchi, and E. Radi, Analytical estimates of the pull-in voltage for carbon nanotubes considering tip-charge concentration and intermolecular forces, Meccanica., vol. 55, no. 1, pp. 193–209, 2020. DOI: 10.1007/s11012-019-01119-8.

[30] J.N. Israelachvili, Intermolecular and Surface Forces, 3rd ed., Elsevier, University of California, Santa Barbara, CA, 2011.

[31] J.T. Chen, H.Z. Liao, and W.M. Lee, An analytical approach for the Green's functions of biharmonic problems with circular and annular domains, J. Mech., vol. 25, no. 1, pp. 59–74, 2009. DOI: 10.1017/S1727719100003609.

[32] S. Wolfram, 2003. The Mathematica Book, 5th ed. Cambridge University Press, Cambridge, UK.

[33] P. Osterberg, M, 1995. Electrostatically actuated microelectromechanical test structures for material property measurement PhD, Thesis Massachusetts Institute of Technology, p.127.

[34] M. Sheploak, and J. Dugundji, Large deflections of clamped circular plates under initial tension and transitions to membrane behavior, J. Appl. Mech., vol. 65, no. 1, pp. 107–115, 1998. DOI: 10.1115/1.2789012.

[35] S.P. Timoshenko, and S. Woinowsky-Krieger, 1959. Theory of Plates and Shells, 2nd ed., McGraw-Hill, New York.

[36] J.A. Voorthuyzen, and P. Bergveld, The influence of tensile forces on the deflection of circular diaphragms in pressure sensors, Sens. Actuat. A., vol. 6, no. 3, pp. 201–213, 1984. DOI: 10.1016/0250-6874(84)80021-9.

[37] I.V. Andrianov, S.G. Koblik, and G.A. Starushenko, Investigation of electrically actuated geometrically nonlinear clamped circular nanoplate, Acta Mech., vol. 235, no. 2, pp. 1015–1026, 2024. DOI: 10.1007/s00707-023-03783-0.

Q3